PERGAMON

Journal of Atmospheric and Solar-Terrestrial Physics 63 (2001) 11–19

Journal of ATMOSPHERIC AND SOLAR-TERRESTRIAL PHYSICS

www.elsevier.nl/locate/jastp

On the chirp-signal structure along the oblique-incidence ionospheric sounding path

N.T. Afanasiev[a], V.P. Grozov[b,*], V.E. Nosov[b], M.V. Tinin[a]

[a] *Research Institute of Applied Physics, Irkutsk State University, 20 Gagarin Blvd., 664003, Irkutsk, Russia*
[b] *Institute of Solar-Terrestrial Physics, Siberian Division of Russia Academy of Science (ISTP SD RAS), P.O. Box 4026, Irkutsk 664033, Irkutsk, Russia*

Received 3 May 1999; received in revised form 23 May 2000; accepted 23 June 2000

Abstract

A theoretical analysis is made of the chirp-ionosonde signal structure for the one- and two-hop propagation in a randomly inhomogeneous ionosphere. For the two-hop propagation, the influence of an additional wave scattering from ground roughnesses is taken into account. A numerical simulation showed that random ionospheric irregularities and ground roughnesses play a significant role in signal structure formation. Numerical simulation results are compared with experimental data obtained for the oblique-incidence ionospheric sounding path.

Keywords: Chirp-ionosond; Ionosphere

1. Introduction

Recent years have witnessed a practical implementation of chirp-ionosondes in ionospheric research, which incorporate such features as good noise immunity, modest power consumption, and high resolution (Barry and Fenwick, 1969; Ivanov et al., 1986; Earl and Ward, 1987; Brynko et al., 1988; Arthur and Cannon, 1994; Lynn, 1998).

Despite the extensive applications of chirp-ionosondes, the structure of chirp-signals is as yet imperfectly understood in the context of their propagation in the ionospheric channel, with due regard for performance characteristics of recording facilities. Past efforts were focused mainly on analyzing the signal structure in the absence of the dispersion in the ionosphere, or by taking into account only the phase dispersion during the propagation in a regular medium, which was associated with the lack of a sufficiently thorough analysis of the chirp-signal structure in random media with allowance made for background refraction (Ilyin et al., 1996; Lundborg and Lungren, 1992; Filipp et al., 1991; Salous, 1989; Barabashov and Vetrogradov, 1994).

It is well known that in the case of oblique-incidence ionospheric soundings the signal at the reception point is generated, on the one hand, through the propagation of the waves directly in the ionosphere without intermediate reflections from the terrestrial surface. On the other hand, the signal can propagate via successive reflections of the waves from the Earth–ionosphere waveguide walls. In this paper, we shall explore both possibilities of formation of a continuous chirp-signal. In the latter case, however, for the sake of simplicity, we will confine ourselves to analyzing the signal behavior at the two-hop propagation.

2. Structure of the one-hop signal

The chirp-ionosonde emits a continuous frequency-modulated signal:

$$V(t) = a_0(t)\mathrm{e}^{-\mathrm{i}(\omega_a t+(\dot{\omega}/2)t^2)}, \tag{1}$$

where ω_a is the initial frequency, $\dot{\omega}$ is the frequency-sweep rate of the signal and $a_0(t)$ is unity throughout the lifetime interval of the signal $V(t)$, and is zero beyond this interval.

* Corresponding author. Fax: +7-3952-462-557.
E-mail address: grozov@iszf.irk.ru (V.P. Grozov).

1364-6826/01/$ - see front matter
PII: S1364-6826(00)00180-2

After the signal has passed through the ionospheric channel, at the receiver input we have

$$U(t) = \int_{-\infty}^{\infty} U_s(\omega, t) e^{-i\omega t}\, d\omega = \int_{-\infty}^{\infty} R(\omega, t) V_s(\omega) e^{-i\omega t}\, d\omega, \quad (2)$$

where $U_s(\omega, t)$ is the spectrum of the received signal, $V_s(\omega)$ is the spectrum of the emitted signal, and $R(\omega, t)$ is the reflection factor from a quasi-stationary ionosphere.

Based on the principle of signal processing in the chirp-ionosonde, it is an easy matter to show that the signal at the ionosonde output will be defined by the expression (Ilyin et al., 1996; Lundborg and Lungren, 1992; Filipp et al., 1991; Vakman, 1963):

$$S(\Omega) = \frac{1}{2\pi}\int_{-\infty}^{\infty} V(t)U^*(t)W(t)e^{i\Omega t}\, dt = \frac{1}{2\pi}\int\int_{-\infty}^{\infty} V_s^*(\omega)R^*(\omega, t)V(t)W(t)e^{it(\omega+\Omega)}\, dt\, d\omega, \quad (3)$$

where $W(t)$ is a weighting function, or a function describing the time "window" of the spectrum analyzer, which in the following, for the sake of simplicity, will be approximated by the expression $W(t) = e^{-(t-t_0)^2/2T^2}$, with T being the duration of the "window".

By taking the square of (3) and averaging over an ensemble of realizations of the random medium, for the mean power spectrum $\langle|S(\Omega)|^2\rangle$ we can obtain:

$$\langle|S(\Omega)|^2\rangle = \frac{1}{(2\pi)^2}\iiiint_{-\infty}^{\infty} V_s(\omega_1)V_s^*(\omega_2)W^*(t_1)W(t_2)V^*(t_1)V(t_2) \times e^{-it_1(\omega_1+\Omega)+it_2(\omega_2+\Omega)}\Gamma(\omega_1, \omega_2, t_1, t_2)\, dt_1\, dt_2\, d\omega_1\, d\omega_2, \quad (4)$$

where $\Gamma(\omega_1, \omega_2, t_1, t_2) = \langle R^*(\omega_1, t_1)R(\omega_2, t_2)\rangle$ is the frequency coherence function of wave field fluctuations in a quasi-stationary ionosphere.

In practice, the duration T is of the order of one second, and the frequency-sweep rate is in the range 50–100 kHz/s. Therefore, it can be assumed that the interval T involves a narrow-band signal, with its spectrum defined as

$$V_s(\omega) = \frac{1}{\sqrt{2\pi\dot{\omega}}}e^{i(\omega-\omega_a)^2/2\dot{\omega}-i(\pi/4)\,\mathrm{sgn}(\dot{\omega})} \times \begin{cases} 1, & \omega_a < \omega < \omega_b, \\ 0, & \omega < \omega_a, \omega > \omega_b. \end{cases} \quad (5)$$

By introducing, when calculating Eq. (4), the summation-difference variables

$$\omega_{1,2} = \omega \pm \frac{\Delta\omega}{2}, \qquad t_{1,2} = t \pm \frac{\Delta t}{2}$$

and taking into account the weak dependence of Γ on t_1, t_2, we obtain

$$\langle|S(\Omega)|^2\rangle = \frac{T\sqrt{\pi}}{(2\pi)^2\dot{\omega}}\int_{-\infty}^{\infty}\varphi_r\left(\omega_0 - \omega - \Omega, \frac{\omega-\omega_0}{\dot{\omega}}, \omega\right) d\omega, \quad (6)$$

where

$$\varphi_r = \frac{1}{2\pi}\int_{-\infty}^{\infty}\int\Gamma(\omega, \Delta\omega, \Delta t)\exp\left\{-\frac{(\Delta t)^2}{4}\dot{\omega}^2T^2 \times\left(1+\frac{1}{\dot{\omega}^2T^4}\right) - \frac{T^2}{4}(\Delta\omega)^2 + \frac{T^2}{2}\dot{\omega}\,\Delta t\,\Delta\omega\right\} \times\exp\left\{i\Delta t(\omega_0-\omega-\Omega)+i\frac{\Delta\omega}{\dot{\omega}}(\omega-\omega_0)\right\} d\Delta\omega\, d\Delta t \quad (7)$$

with $\omega_0 = \omega_a + \dot{\omega}t_0$ being the frequency at $t = t_0$.

For the frequency coherence function of the field, we use the expression obtained in the ray approximation (Afanasiev et al., 1983)

$$\Gamma(\Delta\omega) \cong |A|^2\exp\{i(\Delta\omega\tau + \Delta t\omega_g) - \tfrac{1}{2}(\Delta\omega)^2\sigma_\tau^2\}, \quad (8)$$

where ω_g is the Doppler frequency shift, A is the amplitude, and σ_τ^2 is the dispersion of the propagation time.

Note that in papers of Zernov's group (Gherm et al., 1997a, b) the method of smooth disturbances is used to describe the function of field frequency coherence by taking into account the diffraction effects. In our paper, expression (8) is obtained under conditions of a strong dispersion of the wave phase when diffraction effects make only a slight contribution to the field fluctuations, and the main properties of the field are determined by effects of large-scale irregularities ($..l \gg R_f$, where R_f is the radius of the first Fresnel zone) (Rytov et al., 1978). Substituting Eq. (8) into Eq. (7) and integrating Eq. (6) gives

$$\langle|S(\Omega)|^2\rangle = \frac{A^2T}{2\pi F}\exp\left\{-\frac{(\Omega-\omega_g-\tau(\omega_c))^2}{F^2}\right\}, \quad (9)$$

where τ is the time of signal propagation at the frequency $\omega_c = \omega_0 - \tau(\omega_0)\dot{\omega}$.

$F = \sqrt{\frac{1}{T^2} + 2\dot{\omega}^2\sigma_\tau^2 + (\tau'\dot{\omega}^2T)^2}$ is the "width" of the line observed by the spectrum analyzer at the frequency. $\Omega = \tau(\omega_0)\dot{\omega} + \omega_g$, and $\tau' = (\partial\tau/\partial\omega)(\omega_c)$.

As is evident from formula (9), the resolving power of the chirp-ionosonde is determined by three factors: the band of the "window" of the spectrum analyzer $1/T$; random variations in the propagation time σ_τ^2; and dispersion distortions in the ionosphere (the third term in the radicand for the function F). It is easy to note that by increasing the time of analysis of T, it is possible to decrease the role of the first factor, but the contribution from the second factors remains the same, and the role of the dispersion distortions increases. Generally, however, the role of these distortions counts very little because of the smallness of τ'. Formula (9) was used in

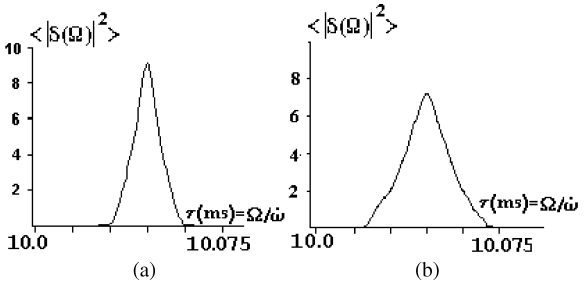

Fig. 1. Results of a numerical simulation of the chirp-signal structure in the case of a one-hop propagation ((a) only the dispersion distortions are taken into account; (b) account is taken of the distortions caused both by the dispersion and by the influence of random ionospheric irregularities).

a numerical simulation of the chirp-signal spectra $\langle|S(\Omega)|^2\rangle$ for one-hop propagation along a path with $D = 3000$ km. Statistical moments of trajectory characteristics were calculated by the technique described in Afanasiev et al. (1989). The model of a regular ionosphere was represented by an exponential dependence of dielectric permittivity on height

$$\varepsilon = 1 - \frac{f_k^2}{f^2} \exp\left\{-\left(\frac{z - z_m}{y_m}\right)^2\right\}. \tag{10}$$

Calculations used parameters typical of the F_2-layer: $Z_m = 270$ km, $Y_m = 80$ km, and $f_k = 7$ MHz. Fig. 1a and b presents the results derived from calculating the chirp-signal spectrum (from here onwards the width of the spectrum analyzer "window" is $T = 1$ s) at one-hop propagation with the inclusion of dispersion distortions (Fig. 1a) and distortions caused both by the dispersion of the medium and by the influence of ionospheric random irregularities (Fig. 1b). Calculations were performed at the frequency $F = 16$ MHz ($F/F_{MUF} = 0.6$), with a chirp-signal frequency variation rate of 100 kHz/s.

Electron density irregularities were characterized by a Gaussian correlation function of dielectric permittivity ($\psi_\varepsilon = v e^{-(\bar{r}_1 - \bar{r}_2)^2/l^2}$, where v is the intensity, and l the irregularity scale), describing the dependence of density fluctuations at space-difference points with coordinates, $\bar{r}_1, \bar{r}_2$. As expected (see formula (10)), the scattering of the radio waves leads to an additional (compared to the influence of the ionospheric dispersion (Lundborg and Lungren, 1992; Filipp et al., 1991) broadening of the signal spectrum. (The irregularity parameters in this case were $v = 10^{-6}$ and $l = 1$ km). An analysis of calculations of the spectra $\langle|S(\Omega)|^2\rangle$ for the other ratios F/F_{MUF} showed that the distortions of the chirp-signal spectrum are determined mainly by the behavior of the radius of frequency correlation of the field of both modes. These, in turn, decrease when the sounding frequency tends to MUF in conditions of a large phase dispersion (intense irregularities) (Tinin et al., 1992). Hence, it follows from theoretical calculations that the width of the chirp-signal spectrum of both modes tends to increase as one approaches the MUF.

3. Structure of the two-hop signal

In the case of a two-hop propagation, the mean power spectrum of the signal at the chirp-ionosonde output can also be determined by expression (9). In doing so, we assume that ground reflection of the waves obeys a specular law, and fluctuations of trajectory characteristics constitute an additive sum of fluctuations of these characteristics at each hop.

Fig. 2a and b presents the envelopes of the chirp-signal spectra for two-hop propagation along the selected path with the same irregularity parameters as in the case of one-hop propagation. The role of random irregularities also manifests itself markedly (see Fig. 2b) in signal structure distortions. Furthermore, the width of the signal spectrum is larger as compared to the one-hop propagation, which is associated with an increase in the length of the scattering area in the ionosphere at two-hop propagation. At the same time, as is evident in some cases in experimental oblique-sounding ionograms (Orlov, 1989), a significant (over 100 μs) broadening of the chirp-signal spectrum at two-hop propagation does not arise here. This inconsistency between theoretical calculations and measurements calls for analysis of alternative reasons for such substantial distortions of the chirp-signal.

In the first place, with the above simulation of the signal structure on the two-hop path, the assumption that the law of mirror reflection of the waves is obeyed at the Earth–ionosphere interface, is questionable. When taking into account the actual lay of the ground, it is necessary to make allowance for the possibility of an additional scattering of ionospheric radio waves (Afanasiev et al., 1990; Tinin et al., 1992), and changes in correlation properties of the HF field would thus be expected. Therefore, a more correct description of the chirp-signal behavior at two-hop propagation requires, strictly speaking, a knowledge of the frequency coherence function of the field $\Gamma(\omega_1, \omega_2)$, with due regard for the scattering from the rough terrestrial surface.

When solving the problem of wave scattering from a rough surface, it is customary to consider (Bass and Fuchs, 1978; Rytov et al., 1978) the case of a regular plane or spherical wave incident on this surface. The problem of ionosphere-reflected HF radio waves scattered from the ground is substantially more complicated because the structure of the incident ionospheric radio wave contains distortions associated with regular refraction and with the scattering of the wave in an inhomogeneous ionosphere. Considering that in the case of multiple-hop propagation the HF scattering from surface roughnesses is essentially in a forward direction, we will take into account mostly large-scale roughnesses which are known (Rytov et al., 1978) to be responsible for the forward scattering. In terms

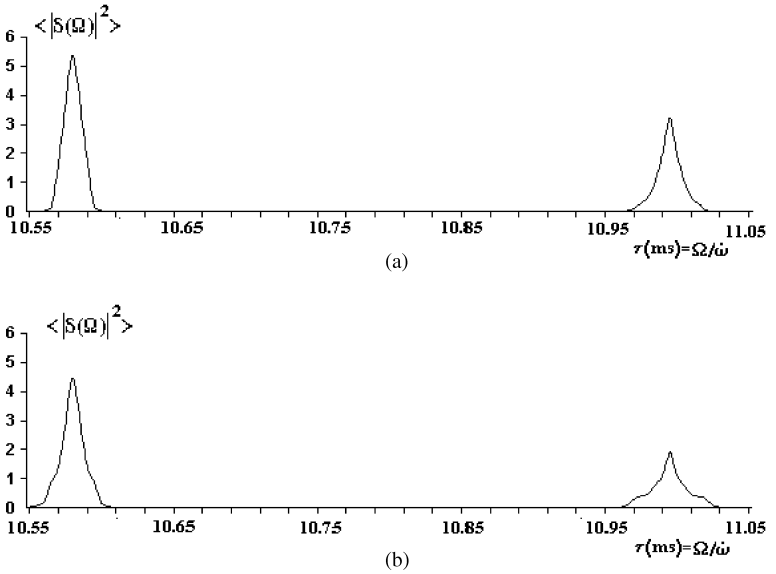

Fig. 2. Results of a numerical simulation of the chirp-signal structure in the case of a two-hop propagation ((a) only the dispersion distortions are taken into account; (b) account is taken of the distortions caused both by the dispersion and by the influence of random ionospheric irregularities).

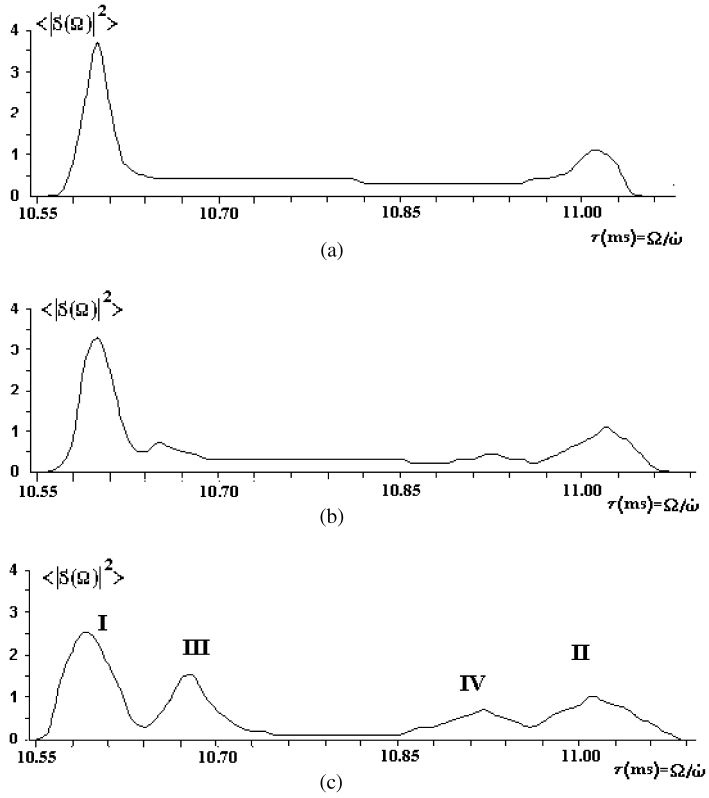

Fig. 3. Results of a numerical simulation of the chirp-signal structure in the case of a two-hop propagation with proper account of the distortions caused both by the dispersion and by the influence of random ionospheric irregularities and ground roughnesses ((a) for the case of the radius of spatial correlation of ground roughness $P = 3$ km; (b), $P = 5$ km, (c), $P = 10$ km).

of such an assumption, the scattering of ionospheric radio waves from the terrestrial surface can be calculated using the Kirchhoff method.

After ground reflection, an expression for the wave field in terms of the Kirchhoff method can be obtained in the form

$$U = \int V_3(r')\frac{\partial}{\partial N}[U_0(r')G(r',r)]\,\mathrm{d}L, \tag{11}$$

where $U_0(r')$ is the incident wave field, $G(r',r)$ the Green's function, N the normal to the rough surface L, and $V_3(r')$ the ground reflection factor.

Further, for the incident wave field and the Green's function we will use the ray approximation and, for the sake of simplicity, we consider the problem of scattering from the ground in a two-dimensional case (neglecting their scattering in the azimuthal plane).

In this case, we have

$$U = -\int V_3 q_z A_0(x')A_g(x',x)\exp\{\mathrm{i}[\Phi_0(x') + \Phi_g(x',x) - q_z\xi(x')]\}\,\mathrm{d}x', \tag{12}$$

where $A_{0,g}$ and $\Phi_{0,g}$ are, respectively, the amplitude and phase of the incident wave and of the Green's function; and q is the wave vector of scattering from the terrestrial surface, $\xi(x')$ is a function characterizing the terrestrial surface roughness.

Assuming that ionospheric irregularities influence predominantly the wave phase and to a lesser extent the wave amplitude (in terms of the ray approximation, this is quite admissible), amplitude fluctuations may be neglected. Using Eq. (12) it is then possible to obtain the expression for the frequency coherence function of the field $\Gamma(\omega_1,\omega_2)$. Assuming that the ray path in the ionosphere encounters a large number of irregularities, i.e. the Gaussian law of phase fluctuation distribution is obeyed, for $\Gamma(\omega_1,\omega_2)$ we have

$$\begin{aligned}\Gamma(\omega_1,\omega_2) = \int\int V_3^2 q_z^2 |A_1(x_1)A_2(x_1,x)|^2 \\ \times\exp\{\mathrm{i}[\Phi_1(x_1,\omega_1 t_1) + \Phi_2(x_1,\omega_1 t_1,x) \\ -\Phi_1(x_2,\omega_2 t_2) - \Phi_2(x_2,\omega_2 t_2)] \\ -\frac{1}{2}\langle[\tilde{\Phi}_1(x_1,\omega_1 t_1) + \tilde{\Phi}_2(x_1,\omega_1 t_1) \\ -\tilde{\Phi}_1(x_2,\omega_2 t_2) - \tilde{\Phi}_2(x_2,\omega_2 t_2) \\ -q_z(\omega_1)\xi(x_1) + q_z(\omega_2)\xi(x_2)]^2\rangle\}\,\mathrm{d}x_1\,\mathrm{d}x_2,\end{aligned} \tag{13}$$

where A_1 and A_2 are the field amplitudes at the first and second hops, respectively. Similarly, Φ_1 and Φ_2 are the values of the field phase of the first and second hops. Upon introducing the summation-difference variables $x_1 - x_2 = \zeta$; $x_1 + x_2 = 2\eta$ and assuming $\omega_2 = \omega_1 + \Delta\omega$, $t_2 = t_1 + \Delta t$, upon integrating we have

$$\Gamma(\omega_1,\omega_2) \cong \sqrt{2\pi}\int \frac{V_3^2 q_z^2 A_1(\eta)|A_2(\eta)^2|\mathrm{e}^{-q_x^2/2\sigma_p^2}L(\eta)\,\mathrm{d}\eta}{\sigma_p}, \tag{14}$$

where

$$L = \exp\left\{-\mathrm{i}\tau'\Delta\omega - \mathrm{i}\omega_g\,\Delta t - \frac{\sigma_\tau'}{2}(\Delta\omega)^2\right\},$$

$$q_z = -k\left[\sqrt{1-S_1^2} + \sqrt{1-S_2^2}\right], \quad q_x = -k(S_1 - S_2),$$

$$S_1 = \sin\beta_{H_1}, \quad S_2 = \sin\beta_{H_2}, \quad \tau' = \tau + \frac{q_x\psi_{x\tau}}{\sigma_p^2},$$

where k is the wave number, and β_{H_1}, β_{H_2} are, respectively, the angles of incidence and reflection of the waves at the end of the first hop,

$$\sigma_\tau'^2 = \sigma_\tau^2 - \frac{\psi_{x\tau}^2}{\sigma_p^2}, \qquad \sigma_\tau^2 = \sigma_{\tau_1}^2 + \sigma_{\tau_2}^2 + \left(\frac{\partial q_z}{\partial\omega}\right)^2\sigma_3^2,$$

$$\sigma_p^2 = \sigma_{\beta_1}^2 + \sigma_{\beta_2}^2 + q_z^2\sigma_{\mathrm{sh}}^2, \qquad \psi_{x\tau} = \psi_{x\tau_1} + \psi_{x\tau_2},$$

where $\sigma_{\tau_1}^2, \sigma_{\tau_2}^2$ are the dispersion of the ray propagation time at the first and second hops, $\sigma_{\beta_1}^2, \sigma_{\beta_2}^2$ the dispersion of angles of arrival of the ray, respectively, at the first and second hops, $\psi_{x\tau_1}, \psi_{x\tau_2}$ the cross-correlation function of fluctuations of the ray propagation range and time at the hops, $\sigma_3^2 = \langle(\xi)^2\rangle$, $\sigma_{\mathrm{sh}}^2 = \langle(\partial\xi/\partial\eta)^2\rangle$ are dispersion of terrestrial surface roughnesses.

On substituting Eq. (14) into Eq. (7) and integrating Eq. (6) for the chirp-signal spectrum on the two-hop path, we have

$$|S(\Omega)|^2 = \frac{T}{\sqrt{2\pi}}\int \frac{V_3^2 q_z^2 A_1|(\eta)A_2(\eta)|^2}{\sigma_p\Theta}\exp\left\{-\frac{q_x^2}{2\sigma_p^2}\right\} \times\exp\left\{-\frac{(\Omega - \omega_g - \tau'\dot{\omega})^2}{\Theta^2}\right\}\mathrm{d}\eta, \tag{15}$$

where $\Theta = \sqrt{1/T^2 + 2\dot{\omega}^2\sigma_\tau'^2 + (\tau'\dot{\omega}^2 T)^2}$.

Expression (15) was used in a numerical simulation of the signal spectrum distortions for different parameters of ionospheric irregularities and terrestrial surface roughnesses. Terrestrial roughnesses were described by a Gaussian correlation function with the parameters μ and p, where $\sqrt{\mu}$ is the standard deviation of the height, and p is the radius of spatial correlation of the terrestrial surface roughness. Fig. 3a–c presents, as a case in point, the results of calculations of $\langle|S(\Omega)|^2\rangle$, where the ionospheric irregularity parameters were as before ($v = 10^{-6}$ and $l = 1$ km), and the value of $\mu = 10^{-2}$ and the scale p took, respectively, the values 10, 5 and 3 km. It is easy to note that a broad temporal plateau (disappearing when roughnesses are smoothed out) appears in the chirp-signal spectrum due to the scattering from ground roughnesses. The plateau dynamics is such

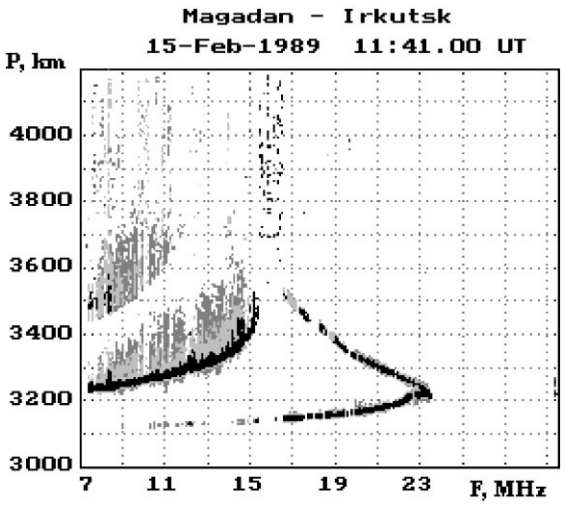

Fig. 4. A typical oblique-incidence ionogram under quiet ionospheric conditions along the Magadan–Irkutsk path.

that with increasing terrestrial surface roughnesses in the chirp-signal spectrum, it transforms into additional modes (see Fig. 3b and c).

A trajectory analysis showed that such modes correspond to combined modes of radio wave propagation. Upon reflection from the ionosphere, the group of lower rays of the first hop, as it is scattered from ground roughnesses, propagates further by the upper path, i.e. it transforms into a group of upper rays of the second hop (see mode III). On the other hand, the group of upper rays of the first hop, after the scattering from the ground, transforms into a group of lower rays of the second hop (see mode IV). Since the energy transported by the lower and upper rays is different because of the large divergence of the upper rays, mode III is energetically more pronounced in the chirp-signal spectrum and, as regards the time delay, is adjacent to fundamental mode I, corresponding to the two-hop propagation by the lower hop. Combined mode IV has a time delay similar to that of fundamental mode II which corresponds to a two-hop propagation by the upper ray. Note that as regards multiple-hop paths, as a result of the multiple wave scattering in the ionosphere and from terrestrial roughnesses, one should expect an increase of the number of additional combined modes that are not associated directly with the regular structure of the ionosphere. This factor must probably be taken into account when solving the problem of predicting the modal composition of distant radio communication signals.

4. Results of experimental investigations

In an effort to make a comparison with the results of the theoretical calculations outlined above, an analysis was made of the experimental data of chirp-sounding for the Magadan–Irkutsk path. The path length is $D = 3000$ km. Performance characteristics of the equipment used are given in Brynko et al. (1988); the frequency-sweep rate was 100 kHz/s, and the sampling duration (duration of the time window) T was 1 s. Runs with a typical structure of ionograms were chosen for processing (see Fig. 4). A total of 100 ionograms were selected (May and October 1989, February 1994 and 1995). The processing was carried out in three steps.

The first step involved a pretreatment and identification of the propagation modes (Grozov et al., 1996). The second step included determining, in the interactive mode, maximum usable frequencies F_{MUF} of the corresponding modes of the received signal. The third step involved determining the duration of the power spectrum τ_{eq} in the frequency range (0.85–1.00) F/F_{MUF} at frequency steps of 94 kHz ($\tau_{\mathrm{eq}} = \delta\Omega/\dot{\omega}$, where $\delta\Omega$ is the width of the power spectrum envelope at the level of $0.5S_{\max}$ or $0.1S_{\max}$). Note that whenever no distortions were present in the ionospheric channel with the selected parameters, $\tau_{\mathrm{eq}} = 30$ μs. For the one-hop and two-hop signals, respectively, τ_{eq} was determined in the automatic and interactive modes.

Fig. 5 presents typical power spectra for the one-hop and two-hop signals (see, respectively, Fig. 5a and b) where the one-hop signal is characterized by the presence of a plateau (a significant increase of τ_{eq} at the $0.1S_{\max}$ level), which is in agreement with the numerical simulation results presented above (see Fig. 3). The determination of $\tau_{\mathrm{eq},i}$ for each ratio F/F_{MUF} is followed by a calculation of the mean value of τ_{eq} ($\tau_{\mathrm{eq,m}} = (1/n)\sum_i \tau_{\mathrm{eq},i}$), where n is the number of values of τ_{eq} obtained at the same value of F/F_{MUF} ($n_{\max} = 100$ is determined by the number of ionograms used). Processing results are given in Figs. 6 and 7.

An analysis of the data obtained shows that for the lower mode 1F (see Fig. 6a) the mean value of τ_{eq} ($\tau_{\mathrm{eq,m}}$) varies from 32 to 39 μs with increasing working frequency. The manner of behavior of $\tau_{\mathrm{eq,m}}$ for both modes corresponds to the variation of the frequency correlation function depending on frequency (Afanasiev et al., 1983).

The two-hop signal shows a stronger increase of $\tau_{\mathrm{eq,m}}$. Also, $\tau_{\mathrm{eq,m}}$, determined at the $0.5S_{\max}$ level, varies from 65 to 88 μs with increasing frequency, and the rate of increase somewhat exceeds that for the one-hop signal (see Fig. 7). In the range (0.98-1) $F/F_{\max}$, $\tau_{\mathrm{eq,m}}$. decreases.

The variation of $\tau_{\mathrm{eq,m}}$, determined at the $0.1S_{\max}$ level, has a more complicated character, and in the frequency range (0.85–1) $F/F_{\max}$ it varies from 213 to 150 ms with increasing frequency (see Fig. 7b). If the character of variation of this quantity is examined over a wider range, then it shows a tendency for the plateau to increase with increasing frequency, and from a certain value, to decrease as one approaches F_{MUF} (see Fig. 8).

In some runs for the two-hop signal, a narrow frequency range shows an effect involving the appearance of additional multipathing. An example of such a situation is given in

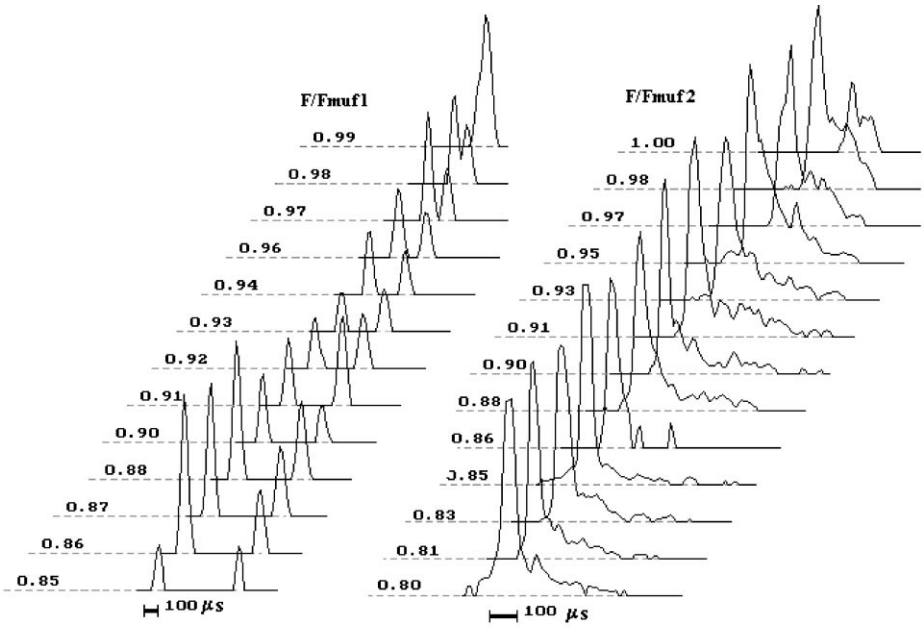

Fig. 5. The form of the power spectrum of chirp-signal depending on the ratio F/F_{MUF} for the case presented in Fig. 4 ((a) form of the power spectrum of the one-hop signal where the lower-mode power spectrum is shown at the left, and the upper-mode power spectrum appears at the right. (b) form of the power spectrum of the two-hop signal).

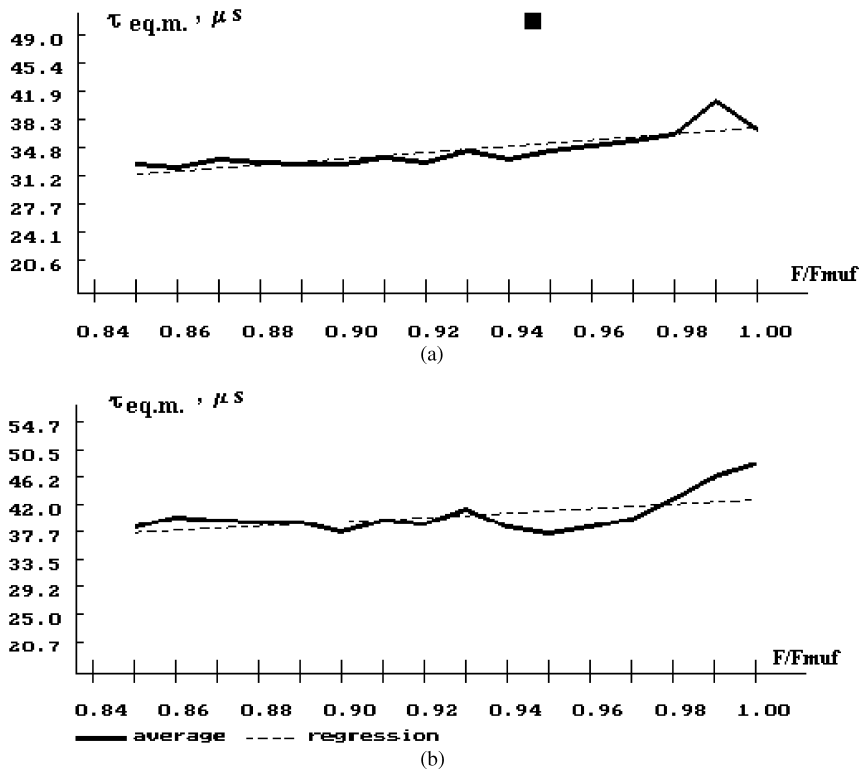

Fig. 6. Experimental dependence of the equivalent length of the power spectrum of the one-hop signal on the ratio F/F_{MUF} ($\tau_{\mathrm{eq,m}} = (1/n)\sum_i \tau_{\mathrm{eq},i}$; $\tau_{\mathrm{eq},i} = \delta\Omega_i/\dot{\omega}$, where $\delta\Omega_i$ is the width of the power spectrum as determined at $0.5S_{\max}$ level for a given ratio F/F_{MUF}; n is the number of counts for a given F/F_{MUF}; $n_{\max} = 100$ and is determined by the number of ionograms used; (a) $\tau_{\mathrm{eq,m}}$ for the lower mode, (b) $\tau_{\mathrm{eq,m}}$ for the upper mode).

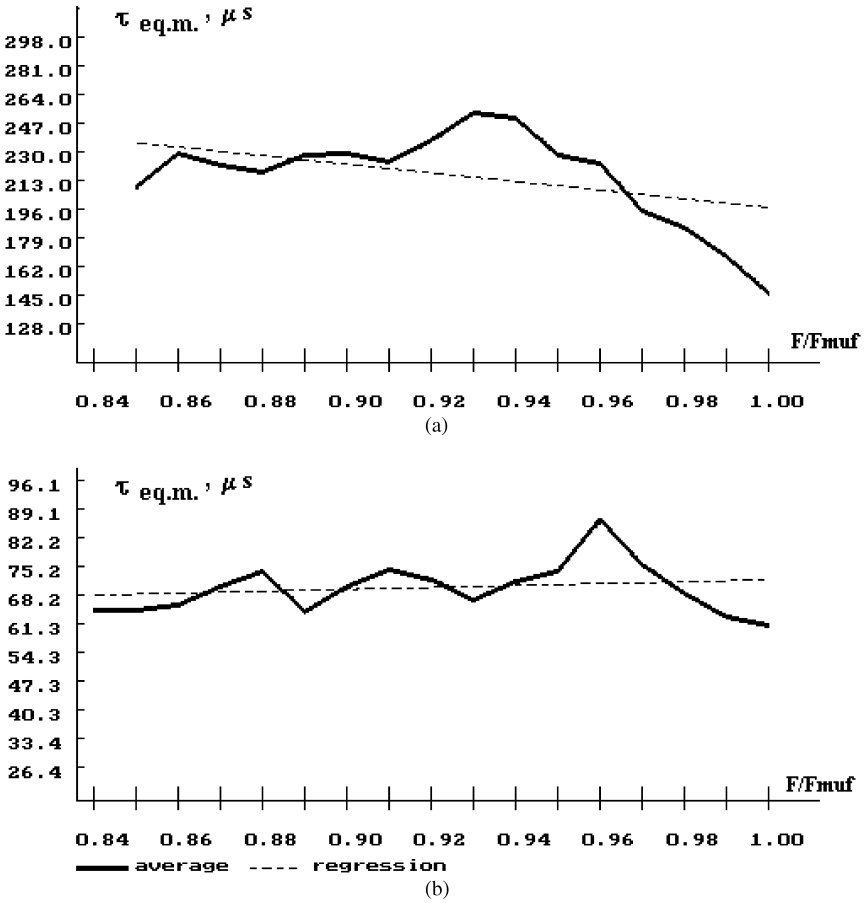

Fig. 7. Experimental dependence of the equivalent length of the power spectrum of the two-hop signal on the ratio F/F_{MUF} ($\tau_{\mathrm{eq,m}} = (1/n)\sum_i \tau_{\mathrm{eq},i}$; $\tau_{\mathrm{eq},i} = \delta\Omega_i/\dot{\omega}$, where $\delta\Omega_i$ is the width of the power spectrum as determined at $0.5S_{\max}$ level for a given ratio F/F_{MUF}; n the number of counts for a given F/F_{MUF}; $n_{\max} = 100$ and is determined by the number of ionograms used; (a) $\tau_{\mathrm{eq,m}}$ determined at $0.5S_{\max}$ level; (b) $\tau_{\mathrm{eq,m}}$ determined at $0.1S_{\max}$ level).

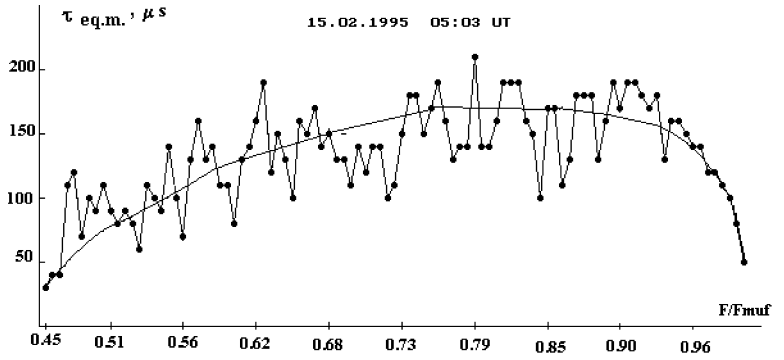

Fig. 8. Experimental dependence of the equivalent length of the power spectrum of the two-hop signal on the ratio F/F_{MUF} over a wide range of frequencies ($F/F_{\mathrm{MUF}} = 0.45$–$0.99$; (.($\tau_{\mathrm{eq,m}} = (1/n)\sum_i \tau_{\mathrm{eq},i}$; $\tau_{\mathrm{eq},i} = \delta\Omega_i/\dot{\omega}$, where $\delta\Omega_i$ is the width of the power spectrum as determined at $0.1S_{\max}$ level for a given ratio F/F_{MUF}; n is the number of counts for a given F/F_{MUF}; $n_{\max} = 100$ and is determined by the number of ionograms used).

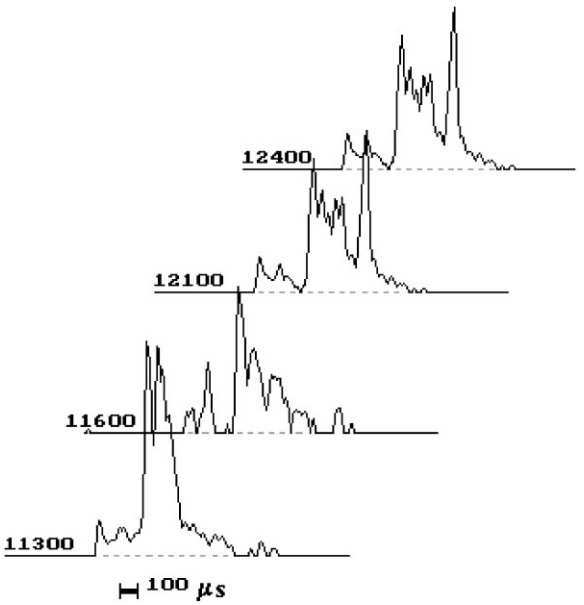

Fig. 9. Example of the appearance of additional multipathing over a narrow range of frequencies.

Fig. 9. This effect that was observed in a numerical simulation (see Fig. 3), is possible in the special event that the path passes over a territory with a mountainous relief, typical of the Irkutsk–Magadan path.

5. Conclusion

Thus, the results of a numerical simulation and experimental data presented above intimate that the proposed technique for calculating the structure of signals emitted by chirp-ionosondes reproduces qualitatively correctly a number of propagation effects caused by the influence of ionospheric irregularities and terrestrial roughness. Also, the main contribution to a change in the signal structure is made by ionospheric irregularities and by terrestrial surface roughnesses, with the latter playing a decisive role for two-hop signals.

Acknowledgements

This work was supported by the Russian Foundation for Basic Research (projects No. 98-02-16023, 97-02-16903).

References

Afanasiev, N.T., Grozov, V.P., Krasikov, A.A., Nosov, V.E., Tinin, V.M., 1983. The frequency correlation function of field fluctuations, and the mean intensity of the pulsed signal during oblique-incidence ionospheric soundings. In: Issledovaniya po geomagnetizmu, aeronomii i fizike Solntsa, Vol. 63. Nauka, Moscow, pp. 180–196.

Afanasiev, N.T., Grozov, V.P., Nosov, V.E., Tinin, M.V., 1989. A software package for computing statistical moments of the HF radio wave field at the oblique propagation. In: Issledo-vaniya po geomagnetizmu, aeronomii i fizike Solntsa, Vol. 84. Nauka, Moscow, pp. 77–80.

Afanasiev, N.T, Pobedina, A.P., Tinin, M.V., 1990. The structure of HF radio wave field at the multiple-hop propagation between an irregular ionosphere and the Earth's rough surface. Abstracts of Papers at the XIV All-Union Conference on Radio Wave Propagation. 4.1. Kharkov, p. 195.

Arthur, P.C., Cannon, P.S., 1994. ROSE: a high performance oblique ionosonde providing new opportunities for ionospheric research. Annali di geofisica XXXVI (2), 135–144.

Barabashov, B.G., Vetrogradov, G.G., 1994. Izvestia. Vuzov. North-Caucasus region. Natural Sciences (3), 39–42.

Barry, G.H., Fenwick, R.B., 1969. In: Jones, T.B. (Ed.), AGARD Conference Proceedings, Vol. 13, p. 487.

Bass, F.G., Fuchs, I.M., 1978. The Wave Scattering From a Statistically Rough Surface. Nauka, Moscow, 264 p.

Brynko, I.G., Galkin, I.A., Grozov, V.P., Dvinskikh, N.I., Nosov, V.E., Matyuoshonok, S.M., 1988. An automatically controlled data gathering and processing system using an FMCW ionosonde. Advances in Space Research 8 (4), (4)121–(4)124.

Earl, G.F., Ward, B.D., 1987. Radio Science 22 (2), 275–297.

Filipp, N.D., Blaunshtein, N.Sh., Erukhimov, L.M. et al., 1991. Current Methods of Investigating Dynamic Processes in the Ionosphere. Shtintsa, Kishinev, 288 p.

Gherm, V.E., Zernov, N.N., Lundborg, B., 1997a. The two-frequency, two-time coherence function for the fluctuating ionosphere: wideband pulse propagation. Journal of Atmospheric and Solar-Terrestrial Physics 59 (14), 1843–1854.

Gherm, V.E., Zernov, N.N., Lundborg, B., Vustberg, A., 1997b. The two-frequency coherence function for the fluctuating ionosphere: narrowband pulse propagation. Journal of Atmospheric and Solar-Terrestrial Physics 59 (14), 1831–1841.

Grozov, V.P., Kurkin, V.I., Nosov, V.I., Ponomarchuk, S.N., 1996. An interpretation of oblique-incidence sounding data using the chirp-signal. Proceedings of ISAP'96, Chiba, Japan, pp. 693–696.

Ilyin, N.V., Khakhinov, V.V., Kurkin, V.I., Nosov, V.E., Orlov, I.I., Ponomarchuk, S.N., 1996. Proceedings of the ISAP'96, Vol. 3, Chiba, Japan, pp. 689–692.

Ivanov, V.A., Frolov, V.A., Shumaev, V.V., 1986. Sounding of the ionosphere with continuous chirp radio signals. Izvestia Vuzov. Radiofizika 29 (2), 235–237.

Lynn, K.S.W., 1998. INAG-62, Sangary, pp. 14–18.

Lundborg, B., Lungren, M., 1992. Journal of Atmospheric and Terrestrial Physics 54 (3/4), 311–321.

Orlov, I.I., 1989. Scientific Report on R&D Topic "Tazgun". Irkutsk 3, 54.

Rytov, S.M., Kravtsov, Yu.A., Tatarsky, V.I., 1978. Introduction to Statistical Radio Physics. Part II. Random Fields. Nauka, Moscow, 464 p.

Salous, S., 1989. Radio Science 24 (4), 585–597.

Tinin, M.V., Afanasiev, N.T., Mikheev, S.M., Pobedina, A.P., 1992. On some problems of the theory of radio wave propagation in a randomly inhomogeneous ionosphere. Radio Science 27 (2), 245–255.

Vakman, D.E., 1963. Composite signals, and the uncertainty principle in radiolocation. Soviet Radio 304.